EurJIC
European Journal of Inorganic Chemistry

A Journal of ChemPubSoc Europe

Accepted Article

Title: Synthesis, structure, photoluminescence, and electroluminescence of four novel europium complexes: Fabrication of pure red organic light emitting diodes from europium complexes

Authors: Sara Karimi Behzad, Mostafa Amini, Mohammad Ghanbari, Mohammad Janghouri, Pavel Anzenbacher Jr, and Seik Weng Ng

To be cited as: *Eur. J. Inorg. Chem.* 10.1002/ejic.201700449

Link to VoR: http://dx.doi.org/10.1002/ejic.201700449

WILEY-VCH

Synthesis, structure, photoluminescence, and electroluminescence of four novel europium complexes: Fabrication of pure red organic light emitting diodes from europium complexes

Sara Karimi Behzad,[a] Mostafa M. Amini,[a,*] Mohammad Ghanbari,[b] Mohammad Janghouri,[c] Pavel Anzenbacher Jr[d,*] and Seik Weng Ng[e]

[a]*Department of Chemistry, Shahid Beheshti University, G.C., Tehran 1983963113, Iran, E-mail: m-pouramini@sbu.ac.ir*

[b]*Department of Organic Chemistry, Faculty of Chemistry, University of Kashan, Kashan, Iran*

[c]*Faculty of Electrical Engineering, Urmia University of Technology, Band Road, Urmia, Iran*

[d]*Department of Chemistry and Center for Photochemical Sciences, Bowling Green State University, Bowling Green, 43403, OH, US, E-mail: pavel@bgsu.edu, http://www2.bgsu.edu/departments/chem/faculty/pavel/*

[e]*School of Pharmacy, University of Nottingham, Malaysia Campus, 43500 Semenyih, Selangor Darul Ehsan, Malaysia*

Supporting information for this article is available on the WWW under http://dx.doi.org/

Abstract

Four novel europium complexes were prepared by reacting europium(III) thenoyltrifluoroacetonate trihydrate with new tridentate ligands based on dipyrazolyl triazine and utilized as emitting materials in electroluminescent devices. The complexes were characterized by elemental analysis, FT-IR spectroscopy, UV-vis spectrophotometery, and ^{1}H NMR spectroscopy. The coordinated ligands serve as light-harvesting chromophores in the complexes with absorption maxima in the range of 334–402 nm [ε= (8.9–81.4) × 10^{3} M^{-1} cm^{-1}]. The ligands efficiently sensitize europium luminescence with maximum quantum yield (Q_L^{Eu}) and observed lifetime (τ_{obs}) values of 34% and 600 μs in the solid state and 35% and 528 μs in toluene, respectively. The radiative lifetimes of Eu ($^{5}D_0$) are in the range of 1170–1281 μs and the ligand-to-metal energy transfer efficiency (η_{sens}) is in the range of 71-92% for those complexes in the solid state and 68-97% for those in solution state. Additionally, organic light emitting diodes (OLEDs) with europium(III) complexes, which exhibited pure red emission, were fabricated. It is shown that by modifying the [Eu(tta)$_3$.3H$_2$O] molecule with ancillary ligands, one can change and control its electroluminescence (EL) spectra along with its electrical properties, such as the current-voltage (J-V) characteristics of OLED devices based on [Eu(tta)$_3$(**L**)]. The best OLED presented a maximum luminance of 3156 cd/m^2 and a maximum efficiency of 0.7 cd/A at an applied voltage of 8 V.

Introduction

In the last decade, a significant amount of research has been devoted to the investigation of photophysical properties of lanthanide complexes owing to their wide-spread applications in the fields of molecular sensing, optoelectronic devices, disease diagnosis, security inks, and biomedical imaging.[1-8] Particularly, the high luminescence efficiencies of lanthanide complexes make them attractive for solid state lighting and electroluminescent display. Most of the lanthanide complexes have narrow emission bandwidths with full width at half maximum (FWHM) smaller than 100 cm^{-1}, making possible the so-called monochromic emission. Among the lanthanide complexes, europium complexes are of considerable interest as electroluminescent red emitters because of their nearly monochromic emission peaks centered at ~612 nm and high electroluminescent efficiency due to the involvement of both triplet and singlet excitons during luminescence.[9-11] In the europium ion, the shielding of the 4f orbital by the closed $5s^2$ and $5p^6$ shells results in narrow line-like emissions of optically pure colors with long lifetimes. Although the luminescence of the europium ion can be efficient, the ion suffers from weak light absorption because the electric dipole f-f transitions that result in light emission from the europium ion are parity-forbidden in spite of the opposite-parity allowed magnetic dipole f-f transitions.[12] One way to overcome the problem of europium ion weak f-f absorption transition and achieve a bright emission is to surround the ion with adequate organic ligands able to harvest light and subsequently transfer the electronic energy to the metal ion excited states, while simultaneously providing a rigid protective coordination shell for minimizing nonradiative deactivation.[3, 5, 13-17] This indirect excitation process is known as the antenna effect or sensitization.[18] It is also desirable that the coordination sphere of europium ion is saturated with ligand and protected from water molecules which strongly bind to the europium and quench its luminescence.[19, 20] It

was proved that the organic ligands have significant effects on the optical and electrical properties of the europium complexes. In order to transfer energy to the europium ion, the ligand must display a suitable excited state. Generally, the first triplet state is responsible for most of the energy transfer,[21, 22] but the singlet-state excitation may also play a non-negligible role.[23]

The luminescent properties of different europium complexes have been widely investigated in the past. As well, many attempts have been made in designing or modifying the ligands of europium complexes to improve molecular recognition ability. In order to improve the carrier transport ability of europium complexes, several research groups attempted to design europium complexes containing organic ligands functionalized with charge carrier transporting groups such as bipyridine derivatives, phenanthroline derivatives, dipyrazolyltriazine, oxadiazole, aryl phosphine oxide,[10] and N-heterocyclic tridentate derivatives. Of these, the development of N-heterocyclic tridentate aromatic ligands is particularly interesting. Several studies on these ligands report the criteria for the formation of stable luminescent complexes by binding of N-heterocyclic tridentate aromatic ligands to $Ln(hfac)_3$ via cascade complexation (hfac = hexafluoroacetylacetonate).[24] More recently, N-heterocyclic tridentate ligands have been used as the building units of multi-tridentate polymers for loading $Ln(hfac)_3$.[25] In pursuit of furthering our understanding of the luminescence properties of lanthanide complexes,[26, 27] we have designed and synthesized a set of europium complexes based on dipyrazolyltriazine and thenoyltrifluoroacetone (tta) as the sensitizing ligands (Scheme 1) in the light of earlier studies.[28-30] We reported here the details of the synthesis, characteristics, and luminescence studies of four new europium complexes [$Eu(tta)_3$(**L**)]. Additionally, red OLED devices were fabricated using these europium complexes and the results are presented and discussed. The fabricated devices have displayed characteristic EL emission bands in the range of 575−710 nm

associated with the europium-centered $^5D_0 \rightarrow {}^7F_J$ (J = 0−4) transitions which give evidence that the antenna effect or sensitization, is operative. Our best device presented a maximum luminance of 3156 cd/m^2 and a maximum efficiency of 0.7 cd/A.

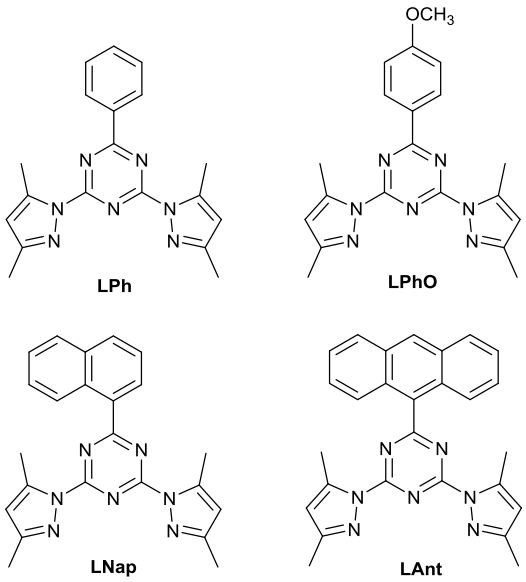

Scheme 1. 2,4-bis(3,5-dimethyl-*1H*-pyrazol-1-yl)-6-aryl-1,3,5-triazine.

Results and Discussion

Synthesis of ligands and complexes

The ligands have been synthesized in three steps (Grignard route) or two steps (Friedel-Crafts route) from cyanuric chloride, aryl or aryl halide, and 3,5-dimethylpyrazole (Scheme 2).

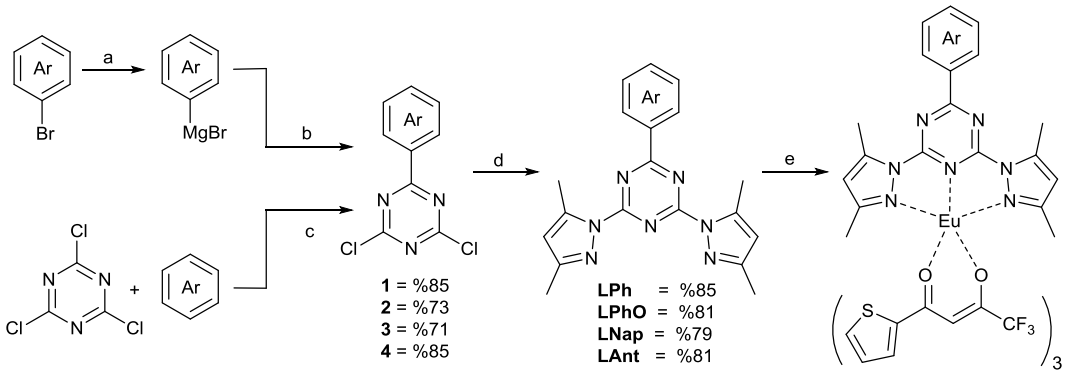

Scheme 2. Synthesis of 2,4-bis(3,5-dimethyl-1H-pyrazol-1-yl)-6-aryl-1,3,5-triazine and their europium complexes. Reaction conditions: (a) bromobenzene or 1-bromonaphthalene,THF, Mg, under N_2, reflux; (b) cyanuric chloride, THF, under N_2, 0 ºC (c) $AlCl_3$, dichloromethane, anthracene or anisole, under N_2 (d) 3,5-dimethylpyrazole, DIPEA, toluene, 80 ºC (e) $[Eu(tta)_3 \cdot 3H_2O]$, THF, r.t.

In the first step of the Grignard route, the aryl-magnesium-bromide (Grignard regent) was formed by reacting the aryl-bromide (bromobenzene or 1-bromonaphthalene) with magnesium metal in THF. In the second step, the Grignard reagent was reacted with cyanuric chloride to produce 2-aryl-4,6-dichloro-1,3,5-triazine with excellent yield after two steps (85% for bromobenzene **1** and 71% for 1-bromonaphthalene **3**). Finally, the ligands (**L**) were obtained by reaction of 2-aryl-4,6-dichloro-1,3,5-triazine with 3,5-dimethylpyrazole in the presence of *N*,*N*-diisopropylethylamine (DIPEA) in toluene at 80 ˚C (Scheme 2). In the first step of the Friedel-Crafts route, the 2-aryl-4,6-dichloro-1,3,5-triazine was formed by reacting cyanuric chloride with arene (anisole **2** or anthracene **4**) in the presence of $AlCl_3$. The final step in the synthesis of ligands (**L**) is the same with the Grignard route. The easy availability of the starting materials and the efficient formation of the ligands under mild conditions with excellent yield are the advantages of this synthetic procedure. The ligands were characterized by ^1H and ^{13}C NMR, Mass spectroscopy and X-ray crystallography. The single crystals of **LPh** and **LAnt** were obtained by crystallization from their dichloromethane solutions and *n*-hexane. Molecular structures of **LPh** and **LAnt** were determined by single crystal X-ray analyses.[31] An ORTEP

drawing with the corresponding atom labeling scheme is displayed in Figure 1. The structure of **LPh** shows a water molecule hydrogen-bonded to the two pyrazole groups.

The reaction of ligands and [Eu(tta)$_3$·3H$_2$O] produces a yellow solution of the europium complexes [Eu(tta)$_3$(**L**)]. The complexes were characterized by ^{1}H NMR spectroscopy and C, H, N-elemental analysis. Unfortunately, all the attempts to obtain single crystals of these complexes were unsuccessful. The nuclear magnetic resonance (^{1}H NMR) spectra of the europium complexes in $CDCl_3$ display highly-symmetrical profiles, which suggest axially symmetric structures with a C_3 axis for the europium complexes. The ^{1}H NMR spectra of such axially symmetric structures was studied by Destri and co-workers and they demonstrated that the structure of the Ln(tta)$_3$ moiety in [Eu(tta)$_3$(**L**)] has a C_3 axis.[32]

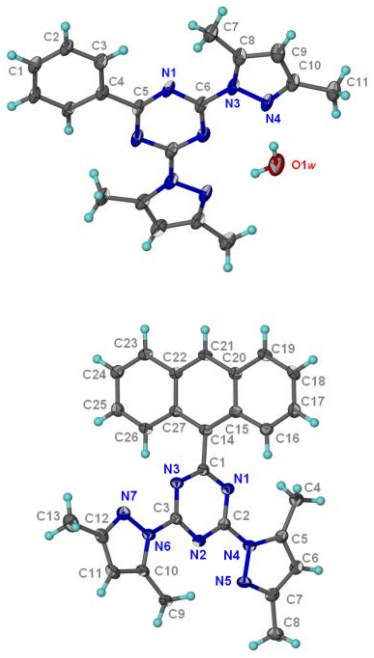

Figure 1. Molecular structures of chromophore ligands: a) **LPh·H$_2$O;** b) **LAnt.**

Photophysical characterization

The optical properties of europium complexes have been studied in both toluene solutions and solid-state. Absorption, steady-state and time-resolved emission spectroscopy, and absolute photoluminescence quantum yields measurements were performed. UV-Vis absorption spectra of the ligands in CH_2Cl_2 and complexes in toluene have been recorded. The corresponding spectra for ligands and their complexes are displayed in Figures S1-S10 of the Supporting Information (SI). The main spectral features are summarized in Table 1.

Table 1. Absorption spectra of the ligands in CH_2Cl_2 and their europium complexes in toluene.[a]

Ligands	**λ_{max}/nm (ε/ 10^3 M^{-1} cm^{-1})**	**Complexes**	**λ_{max}/nm (ε/ 10^3 M^{-1} cm^{-1})**
LPh	272 (72.2)	Eu(tta)$_3$(**LPh**)	350 (40.2)
LPhO	274 (35.3), 305 (29.7)	Eu(tta)$_3$(**LPhO**)	334 (81.4), 350 sh
LNap	270 (47.5), 329 (13.1)	Eu(tta)$_3$(**LNap**)	350 (54.9)
LAnt	368 (11.8), 386 (12.8)	Eu(tta)$_3$(**LAnt**)	350 (54.6), 402 (8.9)

[a] Spectra were recorded at room temperature in the range 250-500 nm. Estimated errors are ±1 nm for λ_{max} and ±5% for ε. The concentration of europium complexes was 10 μM. sh = shoulder.

The ligands display a composite broad absorption band in the UV range corresponding to $\pi\rightarrow\pi^*$ and $n\rightarrow\pi^*$ transitions with a maximum at 270-386 nm and molar absorption coefficients of (11.8-72.2) × 10^3 $M^{-1}cm^{-1}$ and a cut-off between 350 and 440 nm. The maximum is shifted to the lower energies in the order of **LAnt** > **LNap** > **LPhO** > **LPh**. The absorption spectrum of **LPhO** is composed of two main absorption bands at 274 and 305 nm, which can be attributed to the $\pi\rightarrow\pi^*$ and $n\rightarrow\pi^*$ transitions, respectively. The absorption band of **LPh** at 272 nm is associated with the $\pi\rightarrow\pi^*$ transition. Notably, deprived of electron-donating groups, **LPh** did not show any additional low-energy absorption band like **LPhO**. Substitution of the benzene group by naphthalene and anthracene causes a red shift in the lowest energy band in the absorption spectrum. The absorption spectra of the ligand **LNap** displays two main absorption bands at 270

nm and 329 nm, which can be attributed to the π → π* transitions. The absorption spectrum of **LAnt** is composed of several absorption bands with low molar absorption coefficients at 386, 368, and 350 nm, which can also be assigned to the π→π* transitions (Figure S4, SI). The variations observed in the molar absorption coefficients, which exceed the variations expected from the conjugation and push-pull electronic effects, can be attributed to the disparity in the tilting degrees of the plane of the aryl substituents on triazine.

Upon complex formation, the ligand-centered absorption bands maintain red shifts for the maxima and cut-offs, while their intensity increases to (40−81) × 10^3 M^{-1} cm^{-1} as compared to the corresponding free ligands. The absorption spectra of the europium complexes in toluene (10 μM) at room temperature are shown in Figure 2. The low-energy components became more intense in the complexes, presumably due to the overlap between the absorption bands of the tridentate ligands and the *tta* moieties, as evidenced by the presence of shoulders in almost all of the complexes (Table 1, Figure 2, and Figures S6-S10, SI). Furthermore, the complexes also exhibit wider absorption windows as compared to tta, with the red edge extending up to 400 nm.[33] This is mainly due to the polarization of the Eu^{3+} ion, which results in part from the ligand-to-metal charge transfer, thereby decreasing the energy gap. Nevertheless, according to recent studies on [Ln(**L**)$(hfac)_3$], the association constants are in the range of 4 < log(Beta) < 6 in aprotic solvents.[24] Therefore, the electronic spectra (Figure 2 and 3) recorded in dilute solutions might correspond to the photophysical data of the Eu(**L**)$(hfac)_3$ adduct and adduct decomplexation.

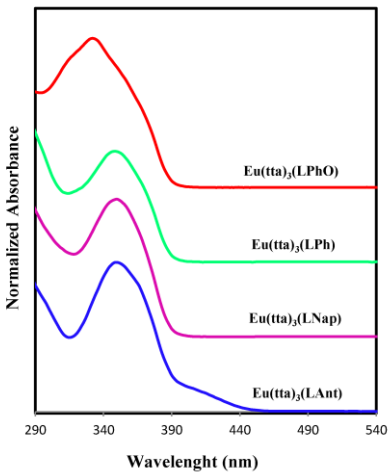

Figure 2. Normalized absorption spectra of europium complexes (10 μM) in toluene.

Photoluminescence properties of complexes

The normalized excitation spectra of the europium complexes in solid state and solution were monitored using the intense band of $^5D_0 \rightarrow {}^7F_2$ transition of the Eu^{3+} ion, and are shown in Figure 3. As expected, the edge of the excitation band for the solids is red shifted compared to the solution. In the solution, the excitation spectra of the complexes show their absorption maxima (λ_{max}) ranging from 336 to 402 nm. In the solid state, the excitation spectra of all complexes display a broad band between 290 and 460 nm (exception is observed for $Eu(tta)_3$(**LAnt**), which exhibit a broad band between 290 and over 510 nm). Also, the complexes show a series of very weak sharp lines characteristic of the Eu^{3+} ion energy level structure. This was assigned to transitions between the $^7F_{0,1}$ and the $^5L_6$, $^5D_{3,2,1}$ levels (Figures 3, solid-state). Notably, the absorptions of the ligands are stronger than the europium f-f absorption transition, and these transitions are overlapped by a broad excitation band. This illustrated that the direct excitation of the europium ion absorption significantly is less efficient than luminescence sensitization through excitation of the ligand. Concomitantly, the broad band can be attributed to

the excited states of ligands or to the ligand-to-metal charge-transfer (LMCT) transitions, which mainly resulted from an interaction between the ligand's first coordination shell and the ion.[13, 34]

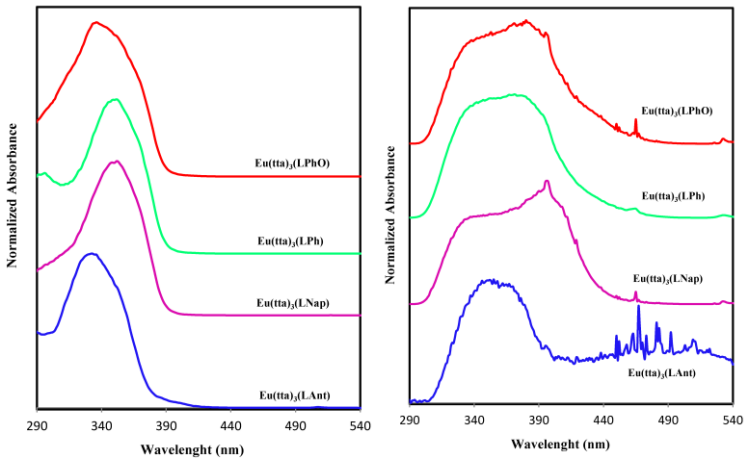

Figure 3. Normalized excitation spectra of $^5D_0$ emission (λ_{max} = 614 nm) of the europium complexes in solution (left) and solid-state (right) at room temperature.

Under ligand excitation, all europium complexes emit red luminescence both in the solid-state and in toluene with a characteristic line-like spectrum in the range of 575-710 nm associated with the europium-centered $^5D_0 \rightarrow {}^7F_J$ (J = 0−4) transitions.[35] The corresponding spectra are shown in Figure 4, while the relevant parameters are listed in Table 2 and Table S1 (SI). Because of overlapping of the ligand centered emission with emission spectra of europium ion and very low overall quantum yield (Q_L^{Eu}) in the [Eu(tta)$_3$(**LAnt**)] complex, the values of photophysical parameters for this complex could not be determined. The europium-centered emission spectra for all complexes are similar (except [Eu(tta)$_3$(**LAnt**)]) and display sharp bands in the solid-state that are broader for toluene solution (Figure 4). The emission spectra of europium complexes did not display the ligand centered transition in the solid-state and solution except [Eu(tta)$_3$(**LAnt**)], suggesting that the ligand transfers the absorbed energy effectively to the emitting level of the europium ion. In the emission spectra, the hypersensitive emission band at 614 nm, $^5D_0 \rightarrow {}^7F_2$, is due to the electric dipole transition, and its corresponding intensity

depends considerably on the geometrical symmetry of the coordination structure and is enhanced in complexes of low symmetry.[36] As previously reported, the intense $^5D_0 \rightarrow {}^7F_2$ band is an indication of a highly polarizable chemical environment around the Eu^{3+} ion and is responsible for the red emission of the europium complexes.[37]

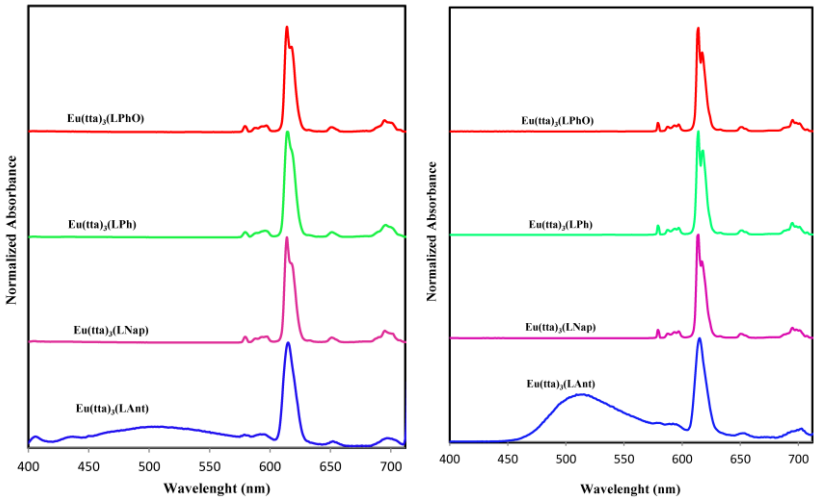

Figure 4. Luminescence spectra (corrected and normalized) of europium complexes in solution (left) and solid-state (right) at room temperature displaying the $^5D_0 \rightarrow {}^7F_J$, J=0-4, transitions; λ_{exc} = 380 nm for solid-state and 360 nm for solution; emission slit: 0.2 nm.

The emission band at 592 nm, $^5D_0 \rightarrow {}^7F_1$, is due to the magnetic dipole transition. Since the magnetic dipole transitions of $^5D_0 \rightarrow {}^7F_1$ are independent of the coordination environment, they can be used as an internal standard to account for ligand differences.[38] The intensity of the electric dipole in all complexes is greater than that of the magnetic dipole, which indicates that the coordination environment of the Eu^{3+} ion does not possess an inversion center. Furthermore, the emission spectra of all complexes display only one band for the $^5D_0 \rightarrow {}^7F_0$ transition and three components for the $^5D_0 \rightarrow {}^7F_1$ transition, reflecting the presence of a single chemical environment around the europium ion. To estimate the relative transition probability of the electric dipole transition, the relative area of the electric dipole ($^5D_0 \rightarrow {}^7F_2$) transition with respect to that of the magnetic dipole ($^5D_0 \rightarrow {}^7F_1$) transition band ($A_{21}$) was evaluated.[39] The A_{21} values for the Eu^{3+}

complexes are listed in Table 2. As already mentioned, the A_{21} parameter in the europium complex reflects the symmetry of the coordination sphere and the distortion of the symmetry around the Eu^{3+} ion enhances the probability of the electric dipole transition.[40] The A_{21} value for all the complexes in the presence of tridentate ligand was considerably large (the A_{21} value is between 11.94-12.33 in solid-state and 12.84-13.14 in solution). This shows the incorporation of a very rigid chelating tridentate ligand into the coordination sphere of the $Eu(tta)_3$ complex resulting in an effective reduction of the symmetry around the Eu^{3+} ion.

Table 2. Absolute quantum yield (Q_L^{Eu}),$^5D_0$ lifetime (τ_{obs}), intrinsic quantum yield (Q_{Eu}^{Eu}), energy transfer efficiency (η_{sens}), the relative integrated intensity of the $^5D_0 \rightarrow {}^7F_2$ transition with respect to that of the $^5D_0 \rightarrow {}^7F_1$ transition band (A_{21}), and radiative (A_{RAD}) and non-radiative (A_{NR}) decay rates for complexes in toluene and solid-state.[a]

Name	Structure	Q_L^{Eu} (%)	τ_{obs} (μs)	τ_{rad} (μs)	Q_{Eu}^{Eu} (%)	η_{sens} (%)	A_{21}	A_{RAD} (s^{-1})	A_{NR} (s^{-1})
$Eu(tta)_3$(**LPh**)	Solid	34	600	1246	48	71	12.33	803	864
	Solution	30	528	1195	44	68	12.84	837	1057
$Eu(tta)_3$(**LPhO**)	Solid	32	551	1281	43	75	11.94	781	1034
	Solution	35	520	1190	44	80	12.93	840	1083
$Eu(tta)_3$(**LNap**)	Solid	24	327	1276	26	92	12.01	784	2275
	Solution	31	375	1170	32	97	13.14	855	1817
$Eu(tta)_3$(**LAnt**)	Solid	1	402	_	_	_	_	_	_
	Solution	2	481	_	_	_	_	_	_

[a] Estimated relative errors: τ_{obs}, ± 2%; Q_L^{Eu}, ± 10%, τ_{rad}, ± 10%; Q_{Eu}^{Eu}, ± 12%; η_{sens}, ± 22%.

To evaluate the efficiency of the Eu^{3+} ion sensitized emission, its 614 nm luminescence decay profiles were obtained in solid-state and solution upon excitation of the ligand absorption band at the maximum of the excitation spectrum. The observed luminescence decays (τ_{obs}) for all the europium complexes are well fitted by a single-exponential function in all media, which indicates the presence of only one emissive Eu^{3+} ion center in each case. The observed lifetime values are 327-600 μs in solid-state and 375-528 μs in solution (Table 2). The typical decay

profiles for all samples are shown in Figure S11. The results of the luminescence lifetime measurements are in accordance with the absence of water in the inner coordination sphere of europium and suggest that the europium ion is well shielded from nonradiative deactivation by the ligands. Relatively longer lifetimes have been observed in the solid-state for the complexes [Eu(tta)$_3$(**LPh**)] (τ_{obs} = 600μs) and [Eu(tta)$_3$(**LPhO**)] (τ_{obs} = 551μs), while the [Eu(tta)$_3$(**LPhNap**)] displayed a shorter lifetime (τ_{obs} = 327 μs). This is presumed to be due to the less prominent nonradiative deactivation pathways (A_{NR}, Table 2).

The quantum yield (Q) is an important parameter for assessment of the efficiency of the emission process in luminescent materials. Table 2 gives the absolute quantum yields (Q_L^{Eu}) of the europium complexes in solutions and solid-state. The recorded absolute quantum yields for solid-state are in the range from 34% for [Eu(tta)$_3$(**LPh**)] to 32% for [Eu(tta)$_3$(**LPhO**)], and 24% for [Eu(tta)$_3$(**LNap**)]. [Eu(tta)$_3$(**LAnt**)] displayed a quantum yield of less than 1% indicating an almost complete quenching of the emission. With the exception of [Eu(tta)$_3$(**LPh**)], the absolute quantum yields values of the complexes recorded in toluene are higher compared to the corresponding solid-state quantum yields (Table 2).

To gain a better understanding of the luminescence efficiencies of all Eu^{3+} complexes, the emission of the europium complexes can be analyzed in terms of Eq.1, where Q_{Eu}^{Eu} is the intrinsic luminescence quantum yield of the Eu ($^5D_0$) level (i.e., obtained upon direct f-f excitation), η_{sens} is the efficiency of the ligand-to-europium energy transfer, τ_{obs} and τ_{rad} are the observed and radiative lifetimes of Eu ($^5D_0$), and the τ_{rad} is the lifetime in the absence of non-radiative deactivation processes:[41]

$$Q_L^{Eu} = \eta_{sens} \times Q_{Eu}^{Eu} = \eta_{sens} \times (\tau_{obs}/\tau_{rad}) \qquad (1)$$

The radiative lifetimes of Eu ($^5D_0$) have been calculated from Eq. 2,[42] where n represents the refractive index of the medium (1.5 for solid-state metal-organic complexes,[43] 1.4969 for toluene), $A_{MD,0}$ is the spontaneous emission probability for the magnetic dipole transition $^5D_0 \rightarrow {}^7F_1$ (14.65 s^{-1}). The I_{tot}/I_{MD} signifies the ratio of the total integrated intensity of the corrected europium emission spectrum to the integrated intensity of the magnetic dipole $^5D_0 \rightarrow {}^7F_1$ transition (Table S1, SI):

$$1/\tau_{rad} = A_{MD,0} \times n^3 \, (I_{tot}/I_{MD}) \qquad (2)$$

The calculated radiative lifetimes are in the narrow range of 1246–1281 μs in the solid-state and 1170–1195 μs in solution. When the complexes are dissolved in toluene, one anticipates finding a longer radiative lifetime for complexes due to the decrease in refractive index (Eq. 2). The measurements, however, showed shorter radiative lifetimes (Table 2), indicating that the inner coordination sphere of the europium ion changes upon dissolution of the complexes in toluene.

To achieve high luminescence in europium complexes, the ligands must protect the europium ion from nonradiative deactivation sources (parameter Q_{Eu}^{Eu}), and provide efficient light harvesting and ligand-to-metal energy transfer (parameter η_{sens}). Because of very low absorption intensity of the f-f transitions, the intrinsic quantum yields of the europium ion (Q_{Eu}^{Eu}) could not be obtained experimentally upon direct excitation.[12] Therefore, the intrinsic quantum yield was calculated from the τ_{obs}/τ_{rad} ratio, which is diagnostic of an environment with minimal non-radiative deactivation processes (Table 2). The calculated values were found to be 26−48%.

With the exception of the ligand containing naphthalene group (η_{sens} ~ 92%), the sensitization efficiencies (η_{sens}) in the solid state calculated from the Q_L^{Eu}/Q_{Eu}^{Eu} ratio are similar. In solution, the η_{sens} values become larger than solid-state thereby resulting in higher overall

quantum yields. The exception was observed for [Eu(tta)$_3$(**LPh**)] (Table 2). The increase of the η_{sens} for the solution measurements can be explained by a spatial rearrangement of a labile ligand-europium binding with respect to the europium ion. This may also be responsible for the broadening of the emission spectra and higher Q_L^{Eu} in solution.

To compare our results with the previously reported results, we adopted the synthesis procedure of [Eu(tta)$_3$] complexes based on dipyrazolyltriazine ligands from literature and synthesized **LPhN** ligand and Eu(tta)$_3$(**LPhN**) complex that have been reported to exhibit the best characteristics (Scheme 3).[28, 44-46]

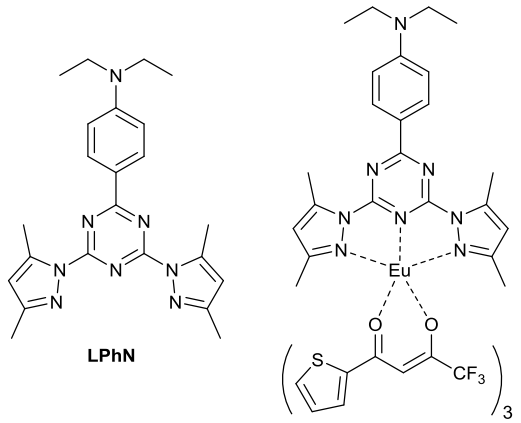

Scheme 3. LPhN ligand and Eu(tta)$_3$(**LPhN**) complex

The photophysical properties of the Eu(tta)$_3$(**LPhN**) complex along with the photophysical properties of the two newly synthesized complexes are summarized in Table 3. According to the photophysical data, the introduction of a strong electron-donating group (-NEt$_2$) on the phenyl ring of the ligand results in a substantial decrease in the quantum yield (Q_L^{Eu}) and observed lifetime (τ_{obs}) of the Eu(tta)$_3$(**LPhN**) complex in the solid state. The absolute Q_L^{Eu} and τ_{obs} of the Eu(tta)$_3$(**LPhN**) complex decrease from 43% and 538 μs, respectively, in toluene to 26% and 374 μs in the solid state (Table 3). In contrast, the emission properties of the remaining

complexes are nearly independent of the medium. With respect to the effect of the ligand structure on the luminescence efficiency of the europium complexes, we observed that the attachment of a -OCH_3 or -$N(CH_2CH_3)_2$ substituent in the *para* position of the phenyl ring decreases the solid state Q_L^{Eu} from 34% for Eu(tta)$_3$**LPh** to 32% and 26% for Eu(tta)$_3$**LPhO** and Eu(tta)$_3$**LPhN**, respectively. In toluene, the Q_L^{Eu} increases from 30% for Eu(tta)$_3$**LPh** to 35% for Eu(tta)$_3$**LPhO** and 43% for Eu(tta)$_3$**LPhN**. Relatively longer lifetimes were observed for the Eu(tta)$_3$(**LPh**) (τ_{obs} = 600 μs) and Eu(tta)$_3$(**LPhO**) (τ_{obs} = 551 μs) in the solid state, while Eu(tta)$_3$(**LPhN**) exhibited a shorter lifetime (τ_{obs} = 374 μs). This is presumed to be due to the more prominent nonradiative deactivation pathways (A_{NR}, Table 3).

Moreover, to compare our results with the previously reported europium complexes based on dipyrazolylpyridine ligands (Scheme 4), the photophysical properties of Eu(**L2**)(hfac)$_3$ and Eu(**L3**)(hfac)$_3$ that have been reported by Piguet and co-workers are summarized in Table 3.[24]

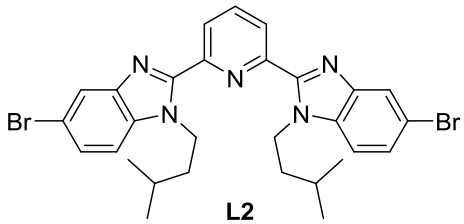

L2

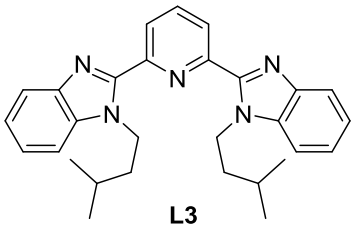

L3

Scheme 4. L2 and L3 ligands [24]

Table 3. Comparison of photophysical properties of the two newly synthesized complexes with Eu(tta)$_3$(**LPhN**).[a]

Name	Structure	Q_L^{Eu} (%)	τ_{obs} (μs)	τ_{rad} (μs)	Q_{Eu}^{Eu} (%)	η_{sens} (%)	A_{RAD} (s^{-1})	A_{NR} (s^{-1})	Ref.
Eu(tta)$_3$(**LPh**)	Solid	34	600	1246	48	71	803	864	This work
	Solution	30	528	1195	44	68	837	1057	This work
Eu(tta)$_3$(**LPhO**)	Solid	32	551	1281	43	75	781	1034	This work
	Solution	35	520	1190	44	80	840	1083	This work
Eu(tta)$_3$(**LPhN**)	Solid	26	374	1222	31	84	818	1807	b
	Solution	43	538	1129	48	90	886	973	b
[Eu(**L2**)(hfac)$_3$]	Solid	29	970	1130	86	34	885	146	[24]
[Eu(**L3**)(hfac)$_3$]	Solid	30	970	1130	86	35	885	146	[24]

[a]Estimated relative errors: τ_{obs}, ± 2%; Q_L^{Eu}, ± 10%, τ_{rad}, ± 10%; Q_{Eu}^{Eu}, ± 12%; η_{sens}, ± 22%. [b]The Eu(tta)$_3$(**PhN**) was synthesized and their photophysical properties were measured

Electroluminescence (EL) characterization of the complexes

In order to attain a proper balance between holes and electrons, their transporting functions must be consolidated into one bipolar host substance. To study the EL properties of the [Eu(tta)$_3$**L**] complexes, light emitting diode (LED) devices were fabricated using [Eu(tta)$_3$(**L)**] in which **L**, the ancillary ligand, acts as the light emitting active layer. The structures of the fabricated devices are as follows –ITO/PEDOT:PSS (45 nm)/CBP:PS (60 nm)/Al (200 nm) and ITO/PEDOT:PSS (45 nm)/CBP:PS (60 nm) [Eu(tta)$_3$(**L**)] (60 nm)/Al (200 nm). The final structure of the device is shown in Figure 5.

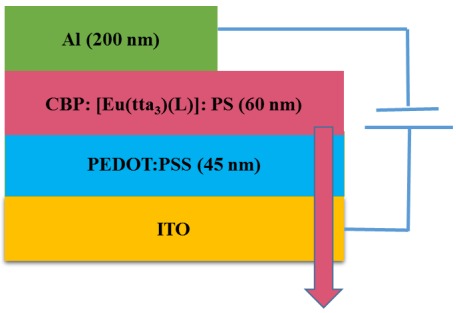

Figure 5. The device structure.

To study the correlation between the EL spectra of the europium complexes and the EL spectra of CBP:PS, an emissive layer without a europium complex was prepared and its EL spectrum was recorded (Figure S12) in order to distinguish the emission of CBP:PS from the emission of the [Eu(tta)$_3$**L**] complexes. The PEDOT-PSS layer can act as a plan arising coating that inhibits electrical short-circuiting and thus improves the lifetime.[47-50] Thus, the usage of an additional PEDOT:PSS layer (45 nm thick) in [Eu(tta)$_3$**L**]-based devices has been investigated. Figure 6 shows the results obtained for an ITO | PEDOT:PSS | Eu complex:CBP:PS| Al device poised at 9 V. As shown in Figure 6, the EL intensity of the devices depended on the ancillary ligand of the europium complex dopants.

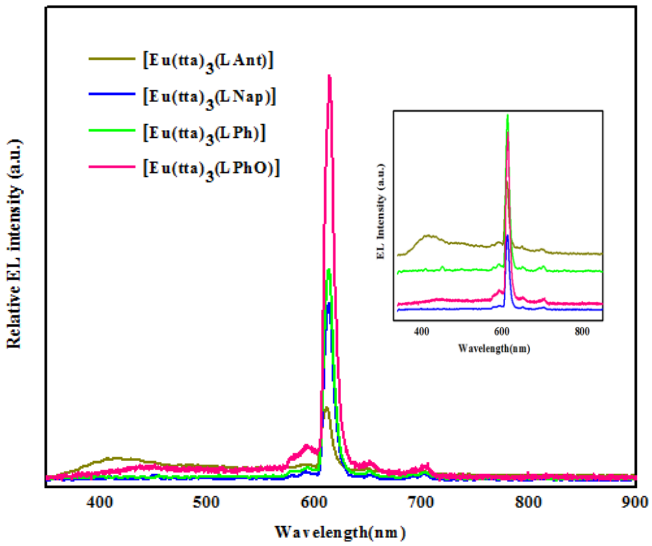

Figure 6. EL spectra of [Eu(tta)$_3$**L**] complexes in CBP:PS blend at 9 V.

The ancillary ligand in the europium complex dopants imposed a low influence on the device color and all the devices exhibited a saturated red chromaticity. In the [Eu(tta)$_3$(**LAnt**)]-based device, the peak at 417 nm is related to CBP:PS and the peaks in the red emission region correspond to the europium complexes. The appearance of the CBP:PS peak indicates that complete energy transfer did not take place from CBP:PS to the [Eu(tta)$_3$(**LAnt**)] molecules. It is evident that the strong emission peak of the host CBP:PS at about 420 nm overlaps with the absorption peak of the europium complexes (Figure 3).

The current-voltage (J-V) characteristics of the devices were also analyzed (Figure S13); a maximum luminance of 3156 cd/m^2 and a maximum efficiency of 0.7 cd/A were obtained with [Eu(tta)$_3$(**LPhO**)]-based OLEDs at an applied voltage of 8 V (Figure S14). The current efficiency increased rapidly up to a certain limit and then decreased as the voltage was increased. The device characteristics of the [Eu(tta)$_3$**L**] complexes are listed in Table S2. The results of the Commission Internationale del'Eclairage (CIE 1931) (X, Y) coordinates of the devices indicated that [Eu(tta)$_3$(**LNap**)] is more red-shifted in comparison with the other complexes (Figure S15). For the [Eu(tta)$_3$(**LNap**)] complex, the full width at half-maximum (FWHM) and color coordinates in the CIE chromaticity at 9 V were 16 nm and (0.67, 0.28), respectively. This implies that we can control the emission properties of the OLED devices by adding different auxiliary ligands.

Conclusions

We have introduced four new tridentate ligands based on dipyrazolyltriazine and developed their easy synthesis from easily accessible starting materials. The ligands readily yielded new mononuclear nine-coordinate neutral complexes [Eu(tta)$_3$**L**] in reaction with Eu(tta)$_3$. Importantly, these ligands very efficiently sensitize the europium luminescence, thereby leading

to absolute quantum yields as large as 34% in the solid state and 35% in toluene. According to the photoluminescence study, the emission spectra of europium complexes did not display the emission broad bands from ligands except [Eu(tta)$_3$(**LAnt**)], which suggest that the ligand transfers the absorbed energy effectively to the emitting level of the europium ion. With respect to the effect of the ligand structure on the luminescence efficiency of europium complexes, we observe that the attachment of a OCH_3 substituent in the *para* position of the phenyl ring decreases the solid state Q_L^{Eu} from 34% for [Eu(tta)$_3$(**LPh**)] to 32% for [Eu(tta)$_3$(**LPhO**)]. In toluene, the Q_L^{Eu} increases from 30% for Eu(tta)$_3$**LPh** to 35% for Eu(tta)$_3$**LPhO**. The variation of the aryl group in the [Eu(tta)$_3$(**LAryl**)] series with Aryl = **Ph**, **Nap**, **Ant**, has an observable effect on Q_L^{Eu} and τ_{obs} in both the solid state and the solution. Thus, [Eu(tta)$_3$(**LPh**)] displays higher Q_L^{Eu} (34%) and τ_{obs} (600 μs) than [Eu(tta)$_3$(**LNap**)] and [Eu(tta)$_3$(**LAnt**)] in the solid state. In the solution [Eu(tta)$_3$(**LPh**)] and [Eu(tta)$_3$(**LNap**)] exhibit the same Q_L^{Eu} but different τ_{obs}. The spatial rearrangement of the ligand with respect to the europium ion as a result of a labile ligand-europium binding may be responsible for the broadening of the emission spectra, the value of the Q_L^{Eu}, shorter radiative lifetime, and increase η_{sens} in toluene. Additionally, we presented the results of OLEDs based on these new europium complexes. The EL spectra of europium complexes illustrated a broad red shift rather than a CBP:PS blend. We observed that the europium emitters change the I-V curve and turn on voltage. The effective overlap between the emission of the host material, CBP:PS, and the absorption of the dopant modulated the EL performance of the europium complexes-doped OLED devices. The best device presented a maximum luminance of 3156 cd/m^2 and a maximum efficiency of 0.7 cd/A of OLEDs at an applied voltage of 8 V. Due to their intense red photo/electroluminescence emissions and good

film forming properties, these novel europium complexes have potential applications as light conversion molecular devices, mainly to fabricate new OLEDs.

Experimental Section

Materials and Instrumentation

The commercially available chemicals were analytical reagent grade and used without further purification. [$Eu(tta)_3{\cdot}3H_2O$] (Purity 95%), 3,5-dimethylpyrazole (98.5%) and *N*,*N* diisopropylethylamine (DIPEA) were purchased from Acros and Merck. PEDOT:PSS (poly(3,4-ethylenedioxythiophene): poly(styrenesulfonate)), PS (polystyrene) and CBP (4,4-N,N-dicarbazole-biphenyl) were obtained from Sigma-Aldrich. All other chemicals were purchased from commercial sources and were used as received unless otherwise mentioned. All solvents were dried and distilled under a nitrogen atmosphere prior to use, according to a standard procedure.[51] Melting points were obtained with an Electrothermal 9200 melting point apparatus and are not corrected. Infrared spectra from 250-4000 cm^{-1} were recorded on a Shimadzu 470 FT-IR instrument with a spectral resolution of 4 cm^{-1}, using KBr pellets. ^1H NMR and ^{13}C NMR spectra were recorded on a Bruker Avance DRX 500 MHz spectrometer or a Bruker Avance 300 MHz spectrometer. Chemical shifts were calibrated to the corresponding deuterated solvents. Mass spectrometry was performed using a Bruker Daltonics Omniflex spectrometer (MALDI-TOF), a Bruker Daltonics autoflex speed spectrometer (MALDI-TOF), and a Finnigan MAT 8430 mass spectrometer at 70 eV. Elemental analyses were performed with a Thermo Finnigan Flash-1112EA microanalyzer. Absorption spectra were measured using a Hitachi U-3010 double beam spectrophotometer at room temperature in the spectral range 250–600 nm. Estimated errors are ±1 nm for λ_{max} and ±5% for ε. Excitation and luminescence spectra were carried out on a single photon counting spectrometer from Edinburgh Analytical Instruments (FL/FS 920) and

were corrected for the instrument function. Luminescence lifetimes were recorded, while monitoring 614 nm Eu(III) $^5D_0 \rightarrow {}^7F_2$ hypersensitive transition on a single photon counting spectrometer from Edinburgh Instrument (FL/FS 920) with a microsecond pulse lamp as the excitation source. The data were analyzed by software supplied by Edinburgh Instruments. The estimated error for the solution and solid-state emission lifetimes is 2%. Spectroscopic studies were conducted in toluene solutions freshly distilled before each experiment; solid-state samples were put into 2 mm i.d. quartz capillaries under air. The absolute quantum yields were measured using a Hamamatsu absolute quantum yield spectrometer C11347. Several measurements were made for each sample, and the results were averaged. Thickness measurements were performed by DekTak 8000; EL of Fabricated OLEDs was performed by USB2000 and HR4000 Ocean Optics. The current–voltage–luminance characteristics measurements were checked by Keithley source meter 2400 model and optical meter Mastech-MS6612.

X-ray Crystallography

Intensity data were collected on a Bruker SMART APEX at 100 K with graphite monochromated *Mo-Kα* radiation to a maximum 2θ value of 27.56° using APEX2 software.[52] The least-squares refinement of diffraction data from 4363 unique reflections was used to obtain cell constants. A numerical absorption correction was performed using SADABS software.[53] The structures were solved by direct method and full-matrix least-square refinement on F^2 with anisotropic displacement parameters was carried out by SHELXL97 crystallographic software package.[54]

Synthesis of Ligands and Complexes

***Synthesis of 2,4-dichloro-6-phenyl-1,3,5-triazine* (1)**

2,4-dichloro-6-phenyl-1,3,5-triazine (**1**) was prepared according to the literature.[55] Briefly, 3.03 g of magnesium turnings (125.0 mmol) were heated to reflux in THF (50 mL) for 30 min.

Afterward, 5.27 mL of bromobenzene (50.0 mmol) in THF (10 mL) were added dropwise through a dropping funnel. The reaction was then heated to reflux for 2 h and cooled. The solution of the Grignard reagent was then added dropwise over 1 h to 9.22 g of cyanuric chloride (50.0 mmol) in THF (50 mL) at 0 ºC and the mixture was stirred overnight in an ice/salt bath. Finally, toluene (50.0 mL) were added and followed by addition of 40.0 mL of 12% HCl. The resulting slurry was extracted twice using ethyl acetate. The separated organic layer was collected and dried over magnesium sulfate. The solvent was removed under reduced pressure, and the light yellow solid was collected by vacuum filtration. The product was dried in a vacuum oven at 100 ºC to give 3.84 g (85%) of high purity product. M.p.: 120-122 ºC. ^{1}H NMR ($CDCl_3$, 300 MHz): δ_H (ppm): 8.51-8.53 (2H, m), 7.65-7.70 (1H, m), 7.49-7.58 (2H, m). FT-IR (KBr, cm^{-1}): 3054, 1716, 1506, 1373, 1247, 848, 771. MS (EI, 70 eV): m/z (%): 226 [M^+, 55], 190 (30), 176 (10), 148 (55), 115 (35), 77 (100).

Synthesis of 2,4-dichloro-6-(4-methoxyphenyl)-1,3,5-triazine (2)

Cyanuric chloride (0.92 g, 5.0 mmol) was dissolved in dichloromethane (25 mL) and then $AlCl_3$ (1.00 g, 7.5 mmol) was added in portions to the solution at room temperature. Anisole, (0.54 mL, 5.0 mmol) was dissolved in dichloromethane (10 mL) and added within 10 minutes at 0 ºC. The resulted black suspension was stirred for 24 h at room temperature. After completion of the reaction, the solvent was removed under reduced pressure, and the residue was dissolved in water (20 mL) and extracted twice (2 × 20 mL) using dichloromethane. The layers were separated, and the organic layer was collected and dried over magnesium sulfate. The solvent was removed under reduced pressure, and the residue was purified by flash column chromatography (hexane/ethyl acetate, 4:1) to give a white solid (0.74 g, 73% yield). M.p.: 134-136 °C. ^{1}H NMR ($CDCl_3$, 300 MHz): δ_H (ppm): 7.88-7.91 (2H, m), 7.09-7.11 (2H, m), 3.87 (1H,

s, OCH_3). FT-IR (KBr, cm^{-1}): 3070, 1515, 1353, 1250, 843. MS (EI, 70 eV): m/z (%): 256 [M^+, 40], 240 (20), 189 (10), 170 (25), 148 (45), 107 (100), 92 (60).

Synthesis of 2,4-dichloro-6-(naphthalen-1-yl)-1,3,5-triazine (3)

Magnesium turnings (3.03 g, 125.0 mmol) were heated to reflux in THF (50 mL) for 30 min. Then 7.02 mL of 1-bromonaphthalene (50.0 mmol) in THF (10 mL) were added dropwise through a dropping funnel. The reaction mixture was then heated to reflux for 2 h and cooled. The Grignard solution was then added dropwise over 1 h to 9.22 g of cyanuric chloride (50.0 mmol) in THF (50 mL) at 0 ºC. The mixture was stirred overnight in an ice/salt bath. Then toluene (50 mL) was added, followed by addition of 40.0 mL of 12% HCl. The resulting slurry was extracted twice using ethyl acetate. The layers were separated, and the organic layer was collected and dried over magnesium sulfate. The solvent was removed under reduced pressure, and the residue was purified by flash column chromatography (hexane/ethyl acetate, 4:1) to give a white solid (9.80 g, 71% yield). M.p.: 170-173 °C. ^{1}H NMR ($CDCl_3$, 300 MHz): δ_H (ppm): 9.10 (1H, d, $^3J_{HH}$= 8.4 Hz), 8.56 (1H, d, $^3J_{HH}$= 7.2 Hz), 8.14 (1H, d, $^3J_{HH}$= 7.8 Hz), 7.96 (1H, d, $^3J_{HH}$= 7.8 Hz), 7.61-7.73 (3H, m). FT-IR (KBr, cm^{-1}): 2928, 2851, 1716, 1527, 1354, 1247, 785. MS (EI, 70 eV): m/z (%): 276 [M^+, 35], 240 (30), 205 (10), 195 (15), 148 (55), 127 (100).

Synthesis of 2-(anthracen-9-yl)-4,6-dichloro-1,3,5-triazine (4)

Cyanuric chloride (500 mg, 2.71 mmol) was dissolved in dichloromethane (15 mL). The solution was cooled down to 0-5 °C and then $AlCl_3$ (0.43 g, 3.25 mmol) was added in portions to the solution. A suspension was formed in which 0.48 g (2.71 mmol) of anthracene were dissolved in dichloromethane (10 mL) and added within 10 minutes. The resulted black suspension was stirred for 2 h at room temperature. After the reaction was completed, the solvent was removed under reduced pressure, and the residue was dissolved in THF (5 mL). To this solution, water

(100 mL) was added, and the precipitate was collected by filtration. The precipitate was washed with water and dried at room temperature to give a pure product (0.75 g, 85%) as a yellow solid. M.p.: 200-202 °C, ^{1}H NMR ($CDCl_3$, 300 MHz): δ_H (ppm): 8.68 (1H, s), 8.08-8.11 (2H, m), 7.81-7.83 (2H, m), 7.54-7.56 (4H, m). FT-IR (KBr, cm^{-1}): 2921, 1702, 1520, 1478, 1254, 848. MS (EI, 70 eV): m/z (%): 326 [M^+, 45], 290 (35), 177 (100), 148 (50), 113 (30).

Synthesis of 2,4-bis(3,5-dimethyl-1H-pyrazol-1-yl)-6-phenyl-1,3,5-triazine (LPh): General procedure (GP1)

A solution of 2,4-dichloro-6-phenyl-1,3,5-triazine (**1**) (656 mg, 2.9 mmol) and *N*,*N* diisopropylethylamine (DIPEA) (1.02 mL, 5.8 mmol) in toluene (30 mL) was heated to 60 ºC and a solution of 3,5-dimethylpyrazole (563 mg, 5.8 mmol) in toluene (10 mL) was added drop-wise. The mixture was stirred at 80 ºC for 24 h and the solvent was then removed under reduced pressure, leaving a solid, which was vigorously shaken for 30 min with water (25 mL). Finally, the solid was filtered, washed with water (20 mL), dried under vacuum and purified by flash column chromatography (hexane/ethyl acetate, 7:3) to give an off-white solid (852 mg, 85% yield). M.p.: 206-208 °C; ^{1}H NMR ($CDCl_3$, 500 MHz): δ_H (ppm): 8.49 (2H, d, $^{3}J_{HH}$= 7 Hz), 7.60 (1H, t, $^{3}J_{HH}$= 7.2 Hz), 7.52 (2H, t, $^{3}J_{HH}$= 7.5 Hz), 6.11 (2H, s, Pz-H), 2.86 (6H, s, Pz-CH_3), 2.36 (6H, s, Pz-CH_3).^{13}C NMR ($CDCl_3$, 125 MHz): δ_H (ppm): 173.9, 164.2, 153.5, 144.5, 135.1, 133.5, 129.3, 128.9, 112.1, 16.4, 14.02. IR (KBr, cm^{-1}): ν = 3429 (H_2O), 2919, 1586, 1533, 1394, 1129, 976, 830, 751, 698. MS (EI, 70 eV): m/z (%): 345 [M^+, 40], 242 (40), 201 (45), 129 (15), 95 (100), 77 (30). MS (MALDI-TOF) 346.26 $[M+H]^+$, 368.25 $[M+Na]^+$. Anal. Calc. for $C_{19}H_{19}N_7$: C, 66.07; H, 5.54; N, 28.39. Found: C, 66.28; H, 5.35; N, 28.28.

Synthesis of 2,4-bis(3,5-dimethyl-1H-pyrazol-1-yl)-6-(4-methoxyphenyl)-1,3,5-triazine (LPhO)

According to **GP1**, 2,4-dichloro-6-(4-methoxyphenyl)-1,3,5-triazine (**2**) (743 mg, 2.9 mmol), DIPEA (1.02 mL, 5.8 mmol) and 3,5-dimethylpyrazole (563 mg, 5.8 mmol) yielded **LPhO** (882 mg, 81%) as an off-white solid after purification by column chromatography (hexane/ethyl acetate, 7:3). M.p.: 216-219 °C; ^{1}H NMR ($CDCl_3$, 500 MHz): δ_H (ppm): 8.49-8.51 (2H, m), 6.98-7.01 (2H, m), 6.09 (2H, s, Pz-H), 3.88 (3H, s, OCH_3), 2.84 (6H, s, Pz-CH_3), 2.35 (6H, s, Pz-CH_3). ^{13}C NMR ($CDCl_3$, 125 MHz): δ_H (ppm): 173.6, 164.1, 164.1, 153.2, 144.4, 131.5, 127.6, 114.2, 111.9, 55.6, 16.2, 14.2. IR (KBr, cm^{-1}): ν = 3396 (H_2O), 2965, 2919, 1593, 1527, 1394, 1261, 1162, 983, 817, 758.MS (EI, 70 eV): m/z (%): 375 [M^+, 35], 344 (55), 280 (30), 268 (40), 107 (60), 95 (100). MS (MALDI-TOF) 376.29 $[M+H]^+$, 398.28 $[M+Na]^+$. Anal. Calc. for $C_{20}H_{21}N_7O$: C, 63.98; H, 5.64; N, 26.12. Found: C, 64.22; H, 5.52; N, 25.95.

Synthesis of 2,4-bis(3,5-dimethyl-1H-pyrazol-1-yl)-6-(naphthalen-1-yl)-1,3,5-triazine (LNap)

According to **GP1**, 2,4-dichloro-6-(naphthalen-1-yl)-1,3,5-triazine (**4)** (801 mg, 2.9 mmol), DIPEA (1.02 mL, 5.8 mmol) and 3,5-dimethylpyrazole (563 mg, 5.8 mmol) yielded **LNap** (906 mg, 79%) as an off-white solid after purification by column chromatography (hexane/ethyl acetate, 7:3). M.p.:168-170 °C; ^{1}H NMR ($CDCl_3$, 500 MHz): δ_H (ppm): 8.89 (1H, d, $^{3}J_{HH}$= 8 Hz), 8.30 (1H, d, $^{3}J_{HH}$= 6.5 Hz), 8.05 (1H, d, $^{3}J_{HH}$= 8 Hz), 7.93 (1H, d, $^{3}J_{HH}$= 7.5 Hz), 7.55-7.60 (3H, m), 6.11 (2H, s, Pz-H), 2.76 (6H, s, Pz-CH_3), 2.37 (6H, s, Pz-CH_3). ^{13}C NMR ($CDCl_3$, 125 MHz): δ_H (ppm):176.2, 163.9, 153.6, 144.7, 134.1, 133.3, 132.8, 131.0, 130.8, 128.8, 127.3, 126.4, 125.9, 125.1, 112.2, 16.1, 14.0. IR (KBr, cm^{-1}): ν = 3425 (H_2O), 3054, 2921, 1527, 1408, 1121, 974, 792. MS (EI, 70 eV): m/z (%): 395 [M^+, 15], 299 (90), 242 (30), 201 (25), 153 (35), 95 (100). MS (MALDI-TOF) 396.28 $[M+H]^+$, 418.26 $[M+Na]^+$. Anal. Calc. for $C_{23}H_{21}N_7$: C, 69.85; H, 5.35; N, 24.79. Found: C, 69.64; H, 5.42; N, 24.98.

Synthesis of 2,4-bis(3,5-dimethyl-1H-pyrazol-1-yl)-6-(naphthalen-1-yl)-1,3,5-triazine (LAnt)

According to **GP1**, 2-(anthracen-9-yl)-4,6-dichloro-1,3,5-triazine (**5)** (946 mg, 2.9 mmol), DIPEA (1.02 mL, 5.8 mmol) and 3,5-dimethylpyrazole (563 mg, 5.8 mmol) yielded **LAnt** (1.05 g, 81%) as a yellow solid after purification by column chromatography (hexane/ethyl acetate, 7:3). M.p.: 217-220 °C; ^{1}H NMR ($CDCl_3$, 500 MHz): δ_H (ppm): 8.60 (1H, s), 8.06 (2H, d, $^{3}J_{HH}$= 8 Hz), 7.90 (2H, d, $^{3}J_{HH}$= 8.5 Hz), 7.44-7.50 (4H, m), 6.09 (2H, s, Pz-H), 2.65 (6H, s, Pz-CH_3), 2.36 (6H, s, Pz-CH_3). ^{13}C NMR ($CDCl_3$, 125 MHz): δ_H (ppm): 177.5, 164.2, 153.9, 145.1, 131.3, 131.1, 129.5, 128.8, 126.8, 125.5, 125.4, 112.4, 16.1, 14.2. IR (KBr, cm^{-1}): ν = 3675 (H_2O), 2925, 1593, 1533, 1394, 1314, 1188, 1096, 963, 830, 738. MS (EI, 70 eV): m/z (%): 445 [M^+, 20], 349 (100), 323 (15), 203 (70), 176 (15), 95 (40). MS (MALDI-TOF) 446.36 $[M+H]^+$, 468.36 $[M+Na]^+$. Anal. Calc. for $C_{27}H_{23}N_7$: C, 72.79; H, 5.20; N, 22.01. Found: C, 72.92; H, 5.30; N, 22.26.

Synthesis of [Eu(tta)$_3$(LPh)] Complex: General Procedure (GP2)

A solution of [Eu(tta)$_3$·3H_2O] (87 mg, 0.1 mmol) in THF (10 mL) was added to a solution of **LPh** (34.5 mg, 0.1 mmol) in THF (10 mL). The mixture was stirred at room temperature for 15 min and then the solvent was removed under reduced pressure, and the residue was redissolved in a small amount of diethyl ether. Addition of *n*-hexane to the solution led to the precipitation of the ternary complex of [Eu(tta)$_3$(**LPh**)] as a yellow powder (101 mg, 87%). M.p.: 122–125 °C; ^{1}H NMR ($CDCl_3$, 500 MHz): δ_H (ppm): 25.46 (6H, s, Pz-CH_3), 12.28 (2H, s, Pz-H), 8.02 (2H, d, $^{3}J_{HH}$= 7.5 Hz, Ph-H), 7.30-7.37 (3H, m, Ph-H), 6.92 (3H, d, $^{3}J_{HH}$= 5.5 Hz, Th-H), 6.01-6.03 (3H, m, Th-H), 5.02 (6H, s, Pz-CH_3), 4.96 (3H, broad, Th-H), -0.43 (3H, broad, CH). IR (KBr, cm^{-1}): ν = 2919, 2853, 1600, 1533, 1314, 1135, 791. Anal. Calc. for $C_{43}H_{31}EuF_9N_7O_6S_3$: C, 44.49; H, 2.69; N, 8.45. Found: C, 44.23; H, 2.67; N, 8.47.

Synthesis of [Eu(tta)$_3$(LPhO)] Complex

According to **GP2**, [Eu(tta)$_3$·3H$_2$O] (87 mg, 0.1 mmol) and **LPhO** (37.5 mg, 0.1 mmol) yielded [Eu(tta)$_3$(**LPhO**)] (102 mg, 86%) as a yellow solid. M.p.: 145-148 °C; ^{1}H NMR ($CDCl_3$, 500 MHz): δ_H (ppm): 25.38 (6H, s, Pz-CH_3), 12.23 (2H, s, Pz-H), 7.90 (2H, d, $^3J_{HH}$= 9.0 Hz, Ph-H), 6.91 (3H, d, $^3J_{HH}$= 5.0 Hz, Th-H), 6.75 (2H, d, $^3J_{HH}$= 9.0 Hz, Ph-H), 6.03 (3H, t, $^3J_{HH}$= 4.0 Hz, Th-H), 4.98 (3H, s, Th-H), 4.95 (6H, s, Pz-CH_3), 3.75 (3H, s, OCH_3), -0.37 (3H, broad, CH). IR (KBr, cm^{-1}): ν = 2932, 2846, 1613, 1507, 1414, 1301, 1135, 784. Anal. Calc. for $C_{44}H_{33}EuF_9N_7O_7S_3$: C, 44.38; H, 2.79; N, 8.23. Found: C, 44.45; H, 2.77; N, 8.28.

Synthesis of [Eu(tta)$_3$(LNap)] Complex

According to **GP2**, [Eu(tta)$_3$·3H$_2$O] (87 mg, 0.1 mmol) and **LNap** (39.5 mg, 0.1 mmol) yielded [Eu(tta)$_3$(**LNap**)] (99 mg, 82%) as a yellow solid. M.p.: 127-132 °C; ^{1}H NMR ($CDCl_3$, 500 MHz): δ_H (ppm): 25.26 (6H, s, Pz-CH_3), 12.20 (2H, s, Pz-H), 8.06 (1H, d, $^3J_{HH}$= 8.0 Hz, Nap-H), 7.75 (2H, d, $^3J_{HH}$= 7.5 Hz, Nap-H), 7.58 (1H, d, $^3J_{HH}$= 7.0 Hz, Nap-H), 7.45 (1H, t, $^3J_{HH}$= 7.0 Hz, Nap-H), 7.36 (2H, dd, $^3J_{HH}$= 7.5 Hz, $^3J_{HH}$= 7.5 Hz, Nap-H), 6.93 (3H, d, $^3J_{HH}$= 4.5 Hz, Th-H), 6.04 (3H, s, Th-H), 5.02 (3H, s, Th-H), 4.87 (6H, s, Pz-CH_3), -0.30 (3H, broad, CH). IR (KBr, cm^{-1}): ν = 2925, 2853, 1600, 1507, 1414, 1295, 1135, 983, 777. Anal. Calc. for $C_{47}H_{33}EuF_9N_7O_6S_3$: C, 46.62; H, 2.75; N, 8.10. Found: C, 46.73; H, 2.77; N, 8.02.

Synthesis of [Eu(tta)$_3$(LAnt) Complex

According to **GP2**, [Eu(tta)$_3$·3H$_2$O] (87 mg, 0.1 mmol) and **LAnt** (44.5 mg, 0.1 mmol) yielded [Eu(tta)$_3$(**LAnt**)] (107 mg, 85%) as an orange solid. M.p.: 135-138 °C; ^{1}H NMR ($CDCl_3$, 500 MHz): δ_H (ppm): 25.07 (6H, s, Pz-CH_3), 12.09 (2H, s, Pz-H), 8.43 (1H, s, Ant-H), 7.89 (2H, d, $^3J_{HH}$= 8.5 Hz, Ant-H), 7.23 (2H, t, $^3J_{HH}$= 8.0 Hz, Ant-H), 6.88 (3H, d, $^3J_{HH}$= 5.5 Hz, Th-H), 6.73 (2H, t, $^3J_{HH}$= 8.0 Hz, Ant-H), 6.56 (2H, d, $^3J_{HH}$= 9.0 Hz, Ant-H), 6.01 (3H, s, Th-H), 4.95 (3H, s,

Th-H), 4.70 (6H, s, Pz-CH_3), -0.22 (3H, broad, CH). IR (KBr, cm^{-1}): ν = 2912, 2846, 1606, 1533, 1420, 1301, 1142, 983, 718. Anal. Calc. for $C_{51}H_{35}EuF_9N_7O_6S_3$: C, 48.58; H, 2.80; N, 7.78. Found: C, 48.42; H, 2.75; N, 7.84.

Preparation of EL devices and testing

Devices with ITO/PEDOT:PSS (45 nm)/CBP:PS (60 nm)/Al (200 nm) and, ITO/PEDOT:PSS (45 nm)/CBP:PS (60 nm) [$Eu(tta)_3$(**L**)] (60 nm)/Al (200 nm) structures were fabricated and the structure of the final sample is illustrated in Figure 5. The fabrication process was initiated by thoroughly washing the ITO-coated glass substrates in an ultrasonic bath with a detergent, acetone, dichloromethane, dichloroethane, ethanol, methanol, in the stated order, and finally rinsing with deionized water. Subsequently, the clean ITO substrate was spin-coated with PEDOT:PSS to obtain 45-nm-thick hole injection layer and baked in an oven for 1 h at 120 ˚C. In the following step, a CBP:PS:dopant (weight ratio of 100:10:3) mixture was dissolved in dichloromethane. In this study, "dopant" refers to each of the four [$Eu(tta)_3$(**L**)] derivatives. This solution was also spin-coated on the previously spin-coated ITO-substrates to obtain a 60-nm-thick matrix layer with emissive dopants. It was baked in the oven for 1 h at 120 ˚C to achieve an even surface and remove any residual solvent. Finally, the aluminum layer is coated on the samples via thermal evaporation in a vacuum environment at a pressure of 10^{-5} mbar to achieve a 200-nm-thick layer.

Acknowledgements

We gratefully acknowledge the financial support from the Research Affairs of Shahid Beheshti University and University of Kashan for supporting this work. One of us (S.K.B) thanks Ministry of Higher Education of Iran for a travel grant to carry out part of her research at Bowling Green

State University. The support from NSF (ECCS-1202439 and DMR-1006761) to P.A. is also gratefully acknowledged.

Keywords: europium • photoluminescence • electroluminescence • OLED • red emission

[1] J.-C. G. Bünzli, S. V. Eliseeva, *Chemical Science* **2013**, *4*, 1939-1949.
[2] S. J. Butler, D. Parker, *Chemical Society Reviews* **2013**, *42*, 1652-1666.
[3] L. Armelao, S. Quici, F. Barigelletti, G. Accorsi, G. Bottaro, M. Cavazzini, E. Tondello, *Coordination Chemistry Reviews* **2010**, *254*, 487-505.
[4] R. Ilmi, K. Iftikhar, *Polyhedron* **2015**, *102*, 16-26.
[5] S. V. Eliseeva, J.-C. G. Bünzli, *Chemical Society Reviews* **2010**, *39*, 189-227.
[6] J.-C. G. Bünzli, *Journal of Luminescence* **2016**, *170*, 866-878.
[7] Z. Ahmed, K. Iftikhar, *Inorganic chemistry* **2015**, *54*, 11209-11225.
[8] G. SanáLim, J. YoungáChang, *Journal of Materials Chemistry C* **2014**, *2*, 10184-10188.
[9] J. Kido, Y. Okamoto, *Chemical Reviews* **2002**, *102*, 2357-2368.
[10] H. Xu, Q. Sun, Z. An, Y. Wei, X. Liu, *Coordination Chemistry Reviews* **2015**, *293*, 228-249.
[11] J. Garcia, M. J. Allen, *European journal of inorganic chemistry* **2012**, *2012*, 4550-4563.
[12] J.-C. G. Bünzli, C. Piguet, *Chemical Society Reviews* **2005**, *34*, 1048-1077.
[13] G. De Sa, O. Malta, C. de Mello Donegá, A. Simas, R. Longo, P. Santa-Cruz, E. Da Silva, *Coordination Chemistry Reviews* **2000**, *196*, 165-195.
[14] M. Reddy, S. Sivakumar, *Dalton Transactions* **2013**, *42*, 2663-2678.
[15] O. Pietraszkiewicz, S. Mal, M. Pietraszkiewicz, M. Maciejczyk, I. Czerski, T. Borowiak, G. Dutkiewicz, O. Drobchak, L. Penninck, J. Beeckman, *Journal of Photochemistry and Photobiology A: Chemistry* **2012**, *250*, 85-91.
[16] J.-C. G. Bünzli, *Coordination Chemistry Reviews* **2015**, *293*, 19-47.
[17] I. G. Fomina, Z. V. Dobrokhotova, V. O. Kazak, G. G. Aleksandrov, K. A. Lysenko, L. N. Puntus, V. I. Gerasimova, A. S. Bogomyakov, V. M. Novotortsev, I. L. Eremenko, *European Journal of Inorganic Chemistry* **2012**, *2012*, 3595-3610.
[18] K. Binnemans, *Chem. Rev.* **2009**, *109*, 4283-4374.
[19] I. Clarkson, R. Dickins, A. de Sousa, *Journal of the Chemical Society, Perkin Transactions 2* **1999**, 493-504.
[20] J. Andres, A. S. Chauvin, *European Journal of Inorganic Chemistry* **2010**, *2010*, 2700-2713.
[21] M. Latva, H. Takalo, V.-M. Mukkala, C. Matachescu, J. C. Rodríguez-Ubis, J. Kankare, *Journal of Luminescence* **1997**, *75*, 149-169.
[22] S. Sato, M. Wada, *Bulletin of the Chemical Society of Japan* **1970**, *43*, 1955-1962.
[23] M.-H. Ha-Thi, J. A. Delaire, V. Michelet, I. Leray, *The Journal of Physical Chemistry A* **2010**, *114*, 3264-3269.
[24] A. Zaïm, H. Nozary, L. Guénée, C. Besnard, J. F. Lemonnier, S. Petoud, C. Piguet, *Chemistry–A European Journal* **2012**, *18*, 7155-7168.
[25] L. Babel, T. N. Y. Hoang, H. Nozary, J. Salamanca, L. Guénée, C. Piguet, *Inorganic Chemistry* **2014**, *53*, 3568-3578.

[26] S. K. Behzad, E. Najafi, M. M. Amini, M. Janghouri, E. Mohajerani, S. W. Ng, *Journal of Luminescence* **2014**, *156*, 219-228.
[27] S. K. Behzad, E. Najafi, M. M. Amini, S. W. Ng, *Monatshefte für Chemie-Chemical Monthly* **2015**, *146*, 571-580.
[28] C. Yang, L. M. Fu, Y. Wang, J. P. Zhang, W. T. Wong, X. C. Ai, Y. F. Qiao, B. S. Zou, L. L. Gui, *Angewandte Chemie International Edition* **2004**, *43*, 5010-5013.
[29] X. Wang, Q. Yan, P. Chu, Y. Luo, Z. Zhang, S. Wu, L. Wang, Q. Zhang, *Journal of Luminescence* **2011**, *131*, 1719-1723.
[30] G.-L. Law, K.-L. Wong, H.-L. Tam, K.-W. Cheah, W.-T. Wong, *Inorganic Chemistry* **2009**, *48*, 10492-10494.
[31] CCDC-1453207-1453208 (LPh and LAnt) contains the supplementary crystallographic data for this paper. These data can be obtained free of charge from The Cambridge Crystallographic Data Centre. www.ccdc.cam.ac.uk/data_request/cif
[32] C. Freund, W. Porzio, U. Giovanella, F. Vignali, M. Pasini, S. Destri, A. Mech, S. Di Pietro, L. Di Bari, P. Mineo, *Inorganic Chemistry* **2011**, *50*, 5417-5429.
[33] N. J. Turro, *Modern molecular photochemistry*, University Science Books, **1991**.
[34] S. S. Braga, R. A. Sá Ferreira, I. S. Gonçalves, M. Pillinger, J. Rocha, J. J. Teixeira-Dias, L. D. Carlos, *The Journal of Physical Chemistry B* **2002**, *106*, 11430-11437.
[35] J.-C. G. Bünzli, *Chem. Rev.* **2010**, *110*, 2729-2755.
[36] C. Görller-Walrand, K. Binnemans, *Handbook on the physics and chemistry of rare earths* **1996**, *23*, 121-283.
[37] M. H. Werts, R. T. Jukes, J. W. Verhoeven, *Physical Chemistry Chemical Physics* **2002**, *4*, 1542-1548.
[38] J.-C. Bünzli, G. R. Choppin, *Lanthanide probes in life, chemical and earth sciences* **1989**, 219.
[39] T. Harada, Y. Nakano, M. Fujiki, M. Naito, T. Kawai, Y. Hasegawa, *Inorganic chemistry* **2009**, *48*, 11242-11250.
[40] A. F. Kirby, D. Foster, F. S. Richardson, *Chemical Physics Letters* **1983**, *95*, 507-512.
[41] N. M. Shavaleev, S. V. Eliseeva, R. Scopelliti, J.-C. G. Bünzli, *Inorganic chemistry* **2014**, *53*, 5171-5178.
[42] A. Aebischer, F. Gumy, J.-C. G. Bünzli, *Physical Chemistry Chemical Physics* **2009**, *11*, 1346-1353.
[43] N. M. Shavaleev, S. V. Eliseeva, R. Scopelliti, J. C. G. Bünzli, *Chem. Eur. J.* **2009**, *15*, 10790-10802.
[44] F. Xue, Y. Ma, L. Fu, R. Hao, G. Shao, M. Tang, J. Zhang, Y. Wang, *Physical Chemistry Chemical Physics* **2010**, *12*, 3195-3202.
[45] W.-S. Lo, W.-M. Kwok, G.-L. Law, C.-T. Yeung, C. T.-L. Chan, H.-L. Yeung, H.-K. Kong, C.-H. Chen, M. B. Murphy, K.-L. Wong, *Inorganic chemistry* **2011**, *50*, 5309-5311.
[46] R. Hao, M. Li, Y. Wang, J. Zhang, Y. Ma, L. Fu, X. Wen, Y. Wu, X. Ai, S. Zhang, *Advanced Functional Materials* **2007**, *17*, 3663-3669.
[47] Y. Cao, G. Yu, C. Zhang, R. Menon, A. Heeger, *Synthetic Metals* **1997**, *87*, 171-174.
[48] T. Brown, J. Kim, R. Friend, F. Cacialli, R. Daik, W. Feast, *Applied Physics Letters* **1999**, *75*, 1679-1681.
[49] K. Y. Lee, Y. K. Kim, O. K. Kwon, J. W. Lee, D. M. Shin, D. Y. Kim, B. C. Sohn, D. S. Choi, *Thin Solid Films* **2000**, *363*, 225-228.

[50] S. Carter, M. Angelopoulos, S. Karg, P. Brock, J. Scott, *Applied Physics Letters* **1997**, *70*, 2067-2069.
[51] D. Perrin, W. Armarego, Pergamon Press: Oxford, **1980**.
[52] SMART, APEX2, version 2.1 (2005) Bruker AXS Inc, Madison
[53] Sheldrich GM (2005) SADABS. University of Gottingen, Germany
[54] (a) Bruker (2008) APEX2 and SAINT. Bruker AXS Inc., Madison, WI; (b) Sheldrick GM (1997) SHELX97. University of Gottingen, Germany.
[55] G. Yu, B. Li, J. Liu, S. Wu, H. Tan, C. Pan, X. Jian, *Polymer Degradation and Stability* **2012**, *97*, 1807-1814.

Table of Content

Synthesis, structure, photoluminescence, and electroluminescence of four novel europium complexes: Fabrication of pure red organic light emitting diodes from europium complexes

Sara Karimi Behzad, Mostafa M. Amini, Mohammad Ghanbari, Mohammad Janghouri,

Pavel Anzenbacher Jr and Seik Weng Ng

Four novel europium complexes based on dipyrazolyl triazine were prepared and utilized as emitting materials in the electroluminescence device. The emission spectra of europium complexes did not display the broadband emission of ligands, and fabricated organic light emitting diodes (OLEDs) with europium(III) complexes showed pure red emission.